

# A MASSIVE CLUSTER OF GALAXIES AT $z = 0.996$

J.-M. Deltorn<sup>1</sup>, O. Le Fèvre<sup>1</sup>

DAEC, Observatoire de Paris-Meudon, 92195 Meudon Cedex, France

David Crampton

Dominion Astrophysical Observatory, National Research Council of Canada, R.R. 5  
Victoria, B.C., V8X4M6, Canada

and

M. Dickinson

Space Telescope Science Institute, Baltimore, MD 21218, USA

## ABSTRACT

We report the identification of a cluster of galaxies around the high-redshift radio galaxy 3CR184 at  $z = 0.996$ . The identification is supported by an excess of galaxies observed in projection in  $I$  band images (both in ground-based and HST data), a peak in the redshift distribution comprising 11 galaxies (out of 56 with measured redshifts) in a  $\sim 2000 \text{ km s}^{-1}$  velocity interval, and the observation on HST WFPC2 frames of a gravitational arc seen projected at  $42h_{50}^{-1}\text{kpc}$  away from the central radio galaxy. We thus have strong evidence for the presence of a massive cluster at  $z \simeq 1$ . The mass contained within the arc radius is in the range  $[1.20 \times 10^{13}h_{50}^{-1}M_{\odot}, 2.78 \times 10^{13}h_{50}^{-1}M_{\odot}]$  for  $z_{arc}$  within the interval 3-1.5; the corresponding mass to light ratio varies from  $56h_{50}$  to  $140h_{50}$ . The velocity dispersion deduced from the galaxy cluster redshifts is  $634_{-102}^{+206}\text{km s}^{-1}$ , leading to a virial mass  $M = 6.16_{-2.40}^{+3.94} \times 10^{14}h_{50}^{-1}M_{\odot}$  and a mass to light ratio  $200h_{50} < (M/L_B)_{400h_{50}^{-1}} < 500h_{50}$  within a radius of  $400h_{50}^{-1}\text{kpc}$ .

*Subject headings:* cosmology: observations – cosmology: large scale structure of universe – galaxies: clusters: general

---

<sup>1</sup>Visiting Astronomer, Canada France Hawaii Telescope. CFHT is operated by the National Research Council of Canada, the Centre National de la Recherche Scientifique of France, and the University of Hawaii.

## 1. INTRODUCTION

Understanding the formation and evolution of large scale structures is of considerable importance to modern cosmology. While galaxy formation and evolution is receiving much warranted attention, the observational study of the formation and evolution of clusters of galaxies or other large scale structures is only now developing.

To identify clusters at high redshifts is a challenging observational task. At low redshifts, one can rely on the projected 2D galaxy density, as was done successfully from the earliest photographic material (e.g., Abell 1958, Zwicky 1961-1968). However, at high redshifts,  $z \geq 0.5$ , it becomes increasingly difficult to identify the 2D galaxy overdensity produced by a cluster because the projected foreground and background galaxies are so numerous that the density contrast is severely reduced and chance alignments of groups of galaxies can mimic the appearance of clusters (Frenk et al. 1990).

The existence of a distant cluster can be proven only if several lines of evidence are combined, which should include the measurement of a projected overdensity of galaxies in few square arcmin area on the sky, combined with a significant overdensity observed in the redshift distribution of galaxies on velocity scales  $\sim 2000 \text{ km s}^{-1}$  in order to reduce the contamination by foreground and background interloper galaxies. In addition, evidence for hot gas, through the detection of X-ray emission, and/or evidence for a peaked mass distribution as indicated by weak or strong lensing of background galaxies, provide strong support for the identification of such overdensities as genuine clusters of galaxies. Although a number of candidates have been proposed, only a few clusters (or proto-clusters) of galaxies have been unambiguously identified at  $z > 0.6$ , with the above criteria fulfilled (Dickinson 1996; Luppino & Kaiser 1996). It is of considerable importance for our knowledge of the evolution of large scale structure to identify more high redshift clusters in order to establish the evolution of their physical properties with redshift.

One possible search strategy is to look for clusters of galaxies around known powerful radio galaxies (Yee & Green 1984; Hill & Lilly 1991; Dickinson 1996; Le Fèvre et al. 1996). We present here the unambiguous identification of a cluster of galaxies around the radio galaxy 3CR184, at a redshift  $z = 0.996$ .

$H_0 = 50 \text{ km s}^{-1} \text{Mpc}^{-1}$  and  $q_0 = 0.5$  are used throughout this *Letter*.

## 2. CFHT IMAGING AND SPECTROSCOPY

The field around 3CR184 was imaged in 1994 January with the Multi-Object-Spectrograph (MOS) at CFHT (Le Fèvre et al 1994) in imaging mode. A 900s image was obtained in the  $R$  band and deep images were also obtained in a narrow band filter centered on  $7480\text{\AA}$  with a bandwidth of  $200\text{\AA}$ , which includes the  $[\text{OII}]\lambda 3727\text{\AA}$  line redshifted to  $z \sim 1$ , for a total integration time of 3600s. Additional  $I$  band images were obtained with the same instrumental setup on 1994 February 6 for a total integration time of 2400s. An initial selection of spectroscopic targets was performed on the basis of excess emission in the narrow band images. Spectroscopic follow-up was performed on 1994 February 6 with MOS in its multi-slit mode. A multi-slit mask with 37 slits, 2 arcseconds in width and at least 10 arcseconds in length each, was used to obtain three spectroscopic exposures of 4800s each. The R300 grism provided a spectral resolution of  $23\text{\AA}$ , and a wavelength coverage from  $5000\text{\AA}$  to  $1\mu\text{m}$ . Data reduction was performed with the MULTIREDD software implemented under IRAF (Le Fèvre et al. 1995). Two galaxies were subsequently identified at a redshift within a few hundred  $\text{km s}^{-1}$  of the radio galaxy, indicating the possible presence of a cluster. Additional spectra were obtained during 1995 December 20-24 with the same instrumental setup as described above. The object selection this time was based purely on the  $I$ -band magnitudes and spatial location on the plane of the sky. Three additional multi-slit masks were used to obtain spectra for 122 objects. Integration times of 15000, 14400, 15000s were obtained for masks 2, 3, and 4, respectively. The linear geometry of the slit positions on each mask result in a selective sampling of galaxies on the sky. All of the objects observed are in an E-W strip of  $8'.5 \times 2'.85$  and the ratio of spectroscopically identified objects to the total number of sampled objects fainter than the radio galaxy ( $I_{RG} = 19.65$ ), and brighter than  $I < 22.2$ , is 0.35 in this strip.

Data processing followed the procedure outlined in Le Fèvre et al. (1995). Of 122 objects observed, 56 were identified as galaxies, 26 turned out to be galactic stars, 1 was identified as a quasar and the remaining 39 were unidentified. A more detailed description of the observational data will be given elsewhere (Deltorn et al. 1997).

## 3. HST IMAGING

HST imaging was conducted with the Wide Field and Planetary Camera 2 during HST cycle 5. A total exposure time of 11000s was obtained with the F814W filter and 6600s with the F606W filter. Exposures were shifted by integral pixel values to allow for cosmic rays and bad pixel cleaning. Standard HST pipeline data reduction was performed. Photometry of 878 objects in the field was obtained, based on the HST photometric zero

point calibration converted to Vega units using the color corrections of Holtzman et al. (1995). The completeness limit is  $I = 26$ , while objects can be detected down to  $I = 28$ . The image of a region  $24 \times 24$  arcsec<sup>2</sup> around the radio galaxy is shown in Figure 1 (Plate 1). Numerous faint galaxies can be seen in the immediate surroundings of the radio galaxy. The radio galaxy and two galaxies with spectroscopically confirmed redshifts which indicate membership in the cluster were imaged in the WFPC2 field; their properties will be discussed elsewhere (Deltorn et al. 1997).

One of the most interesting features in the images is the faint arc-like structure located 4".9 to the north-east of the radio galaxy. The arc is  $\sim 3".6$  long and is visible in both the F606W and the F814W images. Although it is possible that it is due to a chance superposition of several faint galaxies, the center of curvature of the arc is coincident with the radio galaxy and it is unresolved in the radial dimension. The arc has a secure detection  $S/N = 2.8$  in the F814W image and  $S/N = 3.4$  in the F606W filter. The magnitude of the arc is  $I = 25.0 \pm 0.4$  and  $V - I = 0.3 \pm 0.8$ . The presence of this gravitational arc close to the central radio galaxy indicates the proximity of a high concentration of mass.

#### 4. EVIDENCE FOR CLUSTERING AROUND 3CR184 AT $z \sim 0.996$

In order to quantify any projected excess number of galaxies in the vicinity of 3CR184 we have computed density maps using the estimator  $D_{proj}$  defined in Dressler (1980). Cuts in magnitude were applied on the data in order to consider only objects that are fainter than the radio galaxy and brighter than  $I \leq 22.5$  for ground-based images and fainter than the radio galaxy and brighter than  $I \leq 26.5$  for HST data, the latter limiting magnitude corresponding to  $M_B \simeq -17$  at rest, for objects at the redshift of 3CR184. Color selection was also introduced; since high redshift early-type galaxies are on average redder than lower redshift ones we retained only those galaxies with  $R - I \geq 0.2$  for ground-based data and with  $V - I \geq 1$  for the HST data. Those objects should predominantly lie at redshifts greater than 0.5, increasing the projected galaxy density contrast of high redshift structures.

The density maps constructed from the magnitude-limited and the color-limited samples for the HST data show a peak excess density around the radio galaxy corresponding to a  $5\sigma_{bg}$  and  $10\sigma_{bg}$  excess above the mean galaxy background respectively; where  $\sigma_{bg}$  corresponds to the square root of the variance of  $D_{proj}$  measured outside a radius of  $1'$  centered on the radio galaxy. The density peak lies  $6''$  east of the radio galaxy. The ground-based images show lower excess of  $4\sigma_{bg}$  and  $7\sigma_{bg}$  around 3CR184 for the magnitude-limited and the color-limited samples respectively. The central richness,  $N_{0.5}^c$  (Bahcall 1981), was computed after correction for the mean galaxy background estimated

using the deep galaxy counts of Abraham et al. (1996) in the Hubble Deep Field, which led to a central richness of  $N_{0.5}^c \simeq 39 \pm 9$ , the error being calculated assuming purely Poisson statistics. This excess corresponds roughly to an Abell richness class 2 cluster. The significance of the measured excess - far above the statistical “noise” - and the presence of redder objects around the radio galaxy (the excess increasing with the V-I cut), combine to give confidence in the reality of the projected 2D overdensity. Figure 2 shows the redshift distribution of the galaxies in our sample. From a total of 56 securely identified objects, 11 galaxies, including the radio galaxy, have velocities within  $+1198/-750 \text{ kms}^{-1}$  of that of 3CR184. The clear peak at  $z \simeq 1$  apparent in Figure 2 demonstrates the presence of an overdensity in velocity space around 3CR184. The list of galaxies within this peak is given in Table 1. The redshift distribution expected for a similar size sample of field galaxies, as measured from deep redshift surveys (Crampton et al. 1995), indicates that 0.75 galaxies should be observed in a random sample of field galaxies in the same velocity bin, down to  $I \simeq 22$ . It is therefore highly improbable that this excess is due to a random distribution.

The observation of an excess density both in the projected  $(\alpha, \delta)$  space and in redshift space demonstrates unambiguously the reality of the clustering of galaxies around the bright radio galaxy 3CR184. This, combined with the high concentration of mass, as demonstrated by presence of a gravitational arc, secures the identification of a cluster around 3CR184. Future deep X-ray observations of this field would provide useful complementary informations about the hot gaz emission of the cluster.

## 5. VIRIAL AND LENSING MASS ESTIMATES

The observation of a gravitational arc associated with a cluster of galaxies allows a direct determination of the mass within the perimeter defined by the arc. If a spherically-symmetric projected mass distribution is assumed, and the lensed galaxy is coincident with the direction of the cluster center, we have  $M_{proj}(\theta_{arc}) = 0.25c^2G^{-1} \times D_{arc}D_{cl}D_{cl-arc}^{-1}\theta_{arc}^2$ , where  $D_{arc}$ ,  $D_{cl}$  and  $D_{cl-arc}$  are the angular distances from the lensed object, from the cluster, and between the cluster and the lensed galaxy respectively, and  $\theta_{arc} = r_{arc}/D_{cl}$ . We also assume  $r_{arc} \simeq r_c$  ( $r_c$  being the Einstein radius) and the center of mass is taken to be coincident with the radio galaxy. For  $z_{arc}$  in the range 1.5–3, the mass enclosed within  $42h_{50}^{-1}kpc$  from the radio galaxy varies from  $2.78 \times 10^{13}$  to  $1.20 \times 10^{13}h_{50}^{-1}M_{\odot}$ , with an average value of  $1.68 \times 10^{13}h_{50}^{-1}M_{\odot}$ .

If a singular isothermal sphere (SIS) model is adopted, we then have the following central

velocity dispersion:

$$\sigma_{lens} = \left\{ r_{arc} \frac{c^2}{4\pi} \frac{D_{arc}}{D_{cl} D_{cl-arc}} \right\}^{\frac{1}{2}}.$$

This gives  $\sigma_{lens} \in [990, 650] \text{ km s}^{-1}$  for any value of  $z_{arc} \in [1.5, 3]$  (the average value being  $756 \text{ km s}^{-1}$ ), assuming the arc is centered on the radio galaxy. In the framework of SIS approximation, this velocity dispersion is independent of the radius.

The measured redshifts of the cluster galaxies allow derivation of a velocity dispersion in the framework of the cluster. We obtain  $\sigma_{\parallel} = 634_{-102}^{+206} \text{ km s}^{-1}$ , for the sample of eleven galaxies which pass the exclusion criterion of Yahill & Vidal (1977). The errors are estimated from both the redshift uncertainties and the sampling errors due to the small number of galaxies (Danese, De Zotti, di Tullio 1980). This is in good agreement with the velocity dispersion as deduced from the lensing configuration.

Assuming the isotropy, the spherical symmetry of the mass distribution and the dynamical equilibrium of the structure we can derive an estimate of the deprojected virial mass. In the case of equal masses of the galaxies, we found  $M = 6.16_{-2.40}^{+3.94} \times 10^{14} h_{50}^{-1} M_{\odot}$ , the errors being calculated from Danese et al. (1981).

The mass enclosed in a  $1 h_{50}^{-1} \text{ Mpc}$  radius can be estimated within the isothermal sphere approximation. Considering a distribution of galaxies with density profile  $\rho \propto r^{-\epsilon}$ , we have:

$$M(< r) = \frac{\epsilon - 2\beta}{\epsilon - \beta(\epsilon - 1)} \frac{\epsilon \sigma_V^2 r}{G},$$

where  $\beta = 0$  for isotropic orbits and  $\epsilon \simeq 2.2$  (Seldner & Peebles 1977). We find  $M(\sigma_V = 756 \text{ km s}^{-1}, r = 1 h_{50}^{-1} \text{ Mpc}) \simeq 2.97 \times 10^{14} h_{50}^{-1} M_{\odot}$ . Taking the velocity dispersion deduced from the cluster galaxy redshifts leads to a lower value of the mass:  $M(\sigma_V = 634 \text{ km s}^{-1}, r = 1 h_{50}^{-1} \text{ Mpc}) \simeq 2.06 \times 10^{14} h_{50}^{-1} M_{\odot}$ .

The mass to light ratio can be calculated within the radius defined by the arc. The total light within  $4''.9$  from the radio galaxy was corrected from contamination due to field galaxies using the counts of Abraham et al. (1996) and the resulting I magnitude of the cluster population was then converted to  $M_B$ , knowing that I band at a redshift of  $\sim 1$  roughly corresponds to B band at rest, and assuming a no-evolution scenario for the spectral energy distribution of the cluster galaxies. We found a field-subtracted luminosity of  $1.16 \times 10^{12} h_{50}^{-2} L_{B_{\odot}}$ , leading to  $M/L_B \simeq 56 h_{50}$  within  $42 h_{50}^{-1} \text{ kpc}$ . Using the isothermal sphere approximation, we found, after correction for the field galaxies contamination, a total luminosity within  $400 h_{50}^{-1} \text{ kpc}$  of  $L_{400 h_{50}^{-1}} \simeq 2.30 \times 10^{12} h_{50}^{-2} L_{B_{\odot}}$  leading to  $(M/L_B)_{400 h_{50}^{-1}} \simeq 200 h_{50}$ . In addition, if all cluster galaxies are subjected to a luminosity evolution similar to the one measured by the CFRS for field galaxies in the redshift range

$0.75 < z < 1$  (Lilly et al. 1995), the correction to the observed luminosity would give  $M/L_B \simeq 140h_{50}$  within  $42h_{50}^{-1}kpc$  and  $(M/L_B)_{400h_{50}^{-1}} \simeq 500h_{50}$ . We then believe that  $200h_{50} < (M/L_B)_{400h_{50}^{-1}} < 500h_{50}$ . This range is comparable to the higher  $M/L_V^{all}$  found by Smail et al. (1996) for their distant cluster sample ( $z \in [0.17, 0.56]$ ).

## 6. DISCUSSION AND CONCLUSIONS

Our observations of the field around 3CR184 demonstrate unambiguously the presence of a cluster of galaxies, with an associated mass comparable to massive clusters observed locally. We stress that the identification is made possible by a combination of several diagnostics: excess in projected 2D density maps, excess in redshift space, lensing geometry, and mass estimate obtained from virial analysis of spectroscopically measured galaxies. The relative agreement, between the two estimates of the velocity dispersion - from the redshifts and the lensing analysis - converge in describing a quite massive cluster at the redshift of the radio galaxy. We find a lensing mass of  $1.68 \times 10^{13}h_{50}^{-1}M_{\odot}$  within  $42h_{50}^{-1}kpc$ , and derive a virial mass of  $6.16_{-2.40}^{+3.94} \times 10^{14}h_{50}^{-1}M_{\odot}$ . The cluster around 3CR184 is thus one of the very few massive structures yet identified at redshifts larger than 0.9, at epochs when the universe was less than 40% of its present age.

While obtaining velocity dispersion and mass estimate is relatively straightforward, the description of the dynamical state of the cluster is much more uncertain. If a good agreement between virial and lensing masses has been demonstrated for some systems (e.g. PKS 0745-191: Allen, Fabian & Kneib 1996; MS2137-23: Mellier et al. 1993), most arc-cluster associations reveal a significant discrepancy, likely due to the hypothesis involving the mass/velocity dispersion definitions (Miralda-Escudé & Babul 1995; Wu 1996), indicating that these clusters may not be considered as totally relaxed systems. In the case of the cluster around 3CR184, a comparison between the lens and virial velocity dispersions is limited by the limited sample of cluster galaxies, the difficulty in estimating the true center of mass of the presumed cluster, and the simplistic assumptions necessary to derive either  $M$  or  $\sigma$  (either an equilibrium state or a spherical symmetry). Given the current observational dataset it is thus premature to speculate on the similarity between  $\sigma_{lens}$  and  $\sigma_{||}$  to draw any conclusion regarding the dynamical state of the cluster around 3CR184.

The number of high redshift clusters seems to be steadily increasing as observational capabilities become more accute, and the observation of this massive structure at  $z \simeq 1$ , combined with other observations of very high redshift clusters might come to be in

severe conflict with various cosmological models. Recently, the secure identifications of massive bound structures at  $z > 0.8$ , through spectroscopic observation of cluster members (Dickinson 1996; Deltorn et al. 1997, Francis et al. 1996), weak gravitational lensing (Luppino & Kaiser 1996, Smail & Dickinson 1995), or X-ray observations (Luppino & Gioia 1995, Castander et al. 1994) have shown that those structures might not be as rare as predicted by some cosmological scenarios. In CDM and even CHDM models, the number of high redshift massive clusters predicted from both N-body simulations or the Press-Schechter formalism, seems to be too low with respect to observations (Jing & Fang 1994). On the contrary, HDM models predict too many high- $z$ , high- $\sigma_v$  structures (Lijle 1990). Alternatives and modifications to the standard CDM scenario have been advanced in order to account for the emerging data on large scale structure and the amplitude of COBE fluctuations. Among them, low  $\Omega_0$  models (either flat or open) provide a significant number density of massive high redshift clusters that may be compatible with recent observations (Eke, Cole & Frenk 1996; Viana & Liddle 1996 and ref. therein). As the abundance of massive structures provides increasing discrimination with increasing redshift, the identification, without ambiguity, of clusters at  $z \simeq 1$  is now beginning to provide useful observational constraints to the cosmological models.

We thank the CFHT director, P. Couturier for the allocation of discretionary time to start this project, and the CFHT staff for their support during the observations.

## REFERENCES

- Abell, R.G., 1958, ApJS, 3, 211
- Abraham, R.G., Tanvir, N.R., Santiago, B.X., Ellis, R.S., Galzebrook, K., van den Bergh, S., MNRAS, in press
- Allen, S.W., Fabian, A.C., Kneib, J.-P., 1996, MNRAS, 279, 615
- Bahcall, N., 1981, ApJ, 247, 787
- Castander, F.J., Ellis, R.S., Frenk, C.S., Dressler, A., Gunn, J.E., 1994, ApJ, 424, L79
- Crampton, D., Le Fèvre, O., Lilly, S.J., Hammer, F., 1995, ApJ, 455, 96
- Danese, L., De Zotti, G., Giuricin, G., Mardirossian, F., Mezzetti, M. and Ramella M., 1981, ApJ, 244, 777
- Deltorn, J.-M., Le Fèvre, O., Crampton, D., Dickinson, M., 1997, in preparation

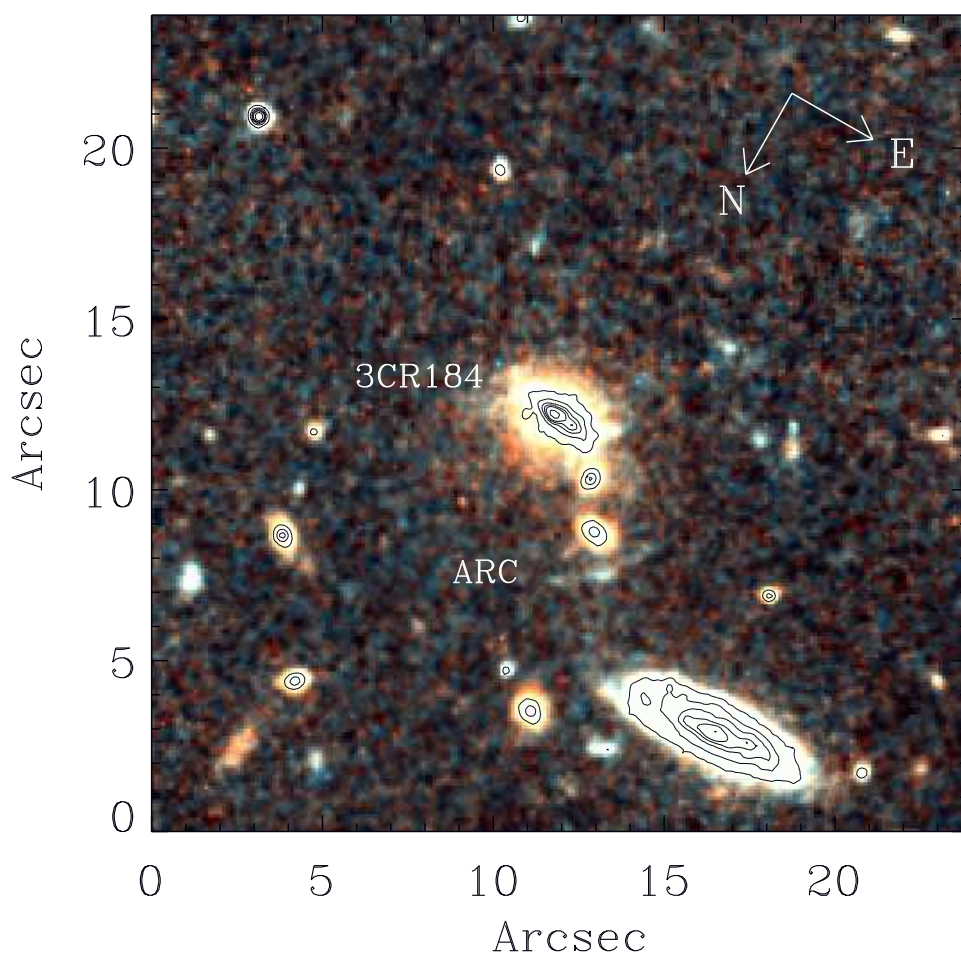


- Dickinson, M., 1996, in “HST and the High Redshift Universe”, World Scientific, eds. N. Tanvir, A. Aragon-Salamanca, and J.V. Wall, in press
- Dressler, A., ApJ, 236, 351
- Eke, V.R., Cole, S., Frenk, C.S., 1996, MNRAS, 282, 263
- Francis, P.J., Woodgate, B.E., Warren, S.J., Moller, P., Mazzolini, M., Bunker, A.J., Lowenthal, J.D., Williams, T.B., Minezaki, T., Kobayashi, Y., Yoshii, Y., 1996, ApJ, 457, 490
- Frenk, C.S., White, S.D.M., Efstathiou, G., Davis, M., 1990, ApJ, 351, 10
- Hill, G.J., Lilly, S.J., 1991, ApJ, 367, 1
- Holtzman, J.A., Burrows, C.J., Casertano, S., Hester, J.J., Trauger, J.T., Watson, A.M., Worthey, G., 1996, PASP, 107, 1065
- Jing, Y.-P., Fang, L.-Z., 1994, ApJ, 432, 438
- Le Fèvre, O., Crampton, D., Felenbok, P., Monnet, G., 1994, A&A, 282, 325
- Le Fèvre, O., Crampton, D., Lilly, S.J., Hammer, F., Tresse, L., 1995, ApJ, 455, 60
- Le Fèvre, O., Deltorn, J.-M., Crampton, D., Dickinson, M., 1996, ApJ, 471, L11
- Lijle, P.B., 1990, ApJ, 351, 1
- Lilly, S.J., Tresse, L., Hammer, F., Crampton, D., Le Fèvre, O., 1995, ApJ, 455, 108
- Luppino, G.A., Gioia, I.M., 1995, ApJ, 445, 77
- Luppino, G.A., Kaiser, N., 1997, ApJ, 475, 20
- Mellier, Y., Fort, B., Kneib, J.-P., 1993, ApJ, 407, 33
- Miralda-Escudé, J., Babul, A., 1995, ApJ, 449, 18
- Seldner, M., Peebles, P.J.E., 1977, ApJ, 215, 703
- Smail, I., Dickinson, M., 1995, ApJ, 455, L99
- Smail, I., Ellis, R.S., Dressler, A., Couch, W.J., Oemler, A., Sharples, R.M., Butcher, H., preprint

- Steidel, C.C., Giavalisco, M., Pettini, M., Dickinson, M., Adelberger, K., 1996, ApJ, in press
- Viana, P.T.P., Liddle, A.R., 1996, MNRAS, 281, 323
- Wu, X.-P., Fang, L.-Z., 1996, ApJ, 467, L45
- Yahill, A., Vidal, N., 1977, ApJ, 214, 347
- Yee, H., Green, 1984, ApJ, 280, 79
- Zwicky, F., Herzoh, E., Wild, P., Karpowicz, M., Kowal, C.T., 1961-1968, Catalogue of Galaxies and Clusters of Galaxies, Pasadena, Calif. Inst. Technol.

Fig. 1.— Sum of the HST F606W and F814W images of a  $24 \times 24$  arcsec<sup>2</sup> field around 3CR184. The arc is located 4''9 north-east of the radio galaxy and extends on 3''6.

Fig. 2.— Redshift distribution of 56 galaxies in the field of 3CR184. The redshifts were obtained from MOS spectroscopy at CFHT. The bin width corresponds to 2000 km s<sup>-1</sup> at the redshift of the radio galaxy (z=0.996).



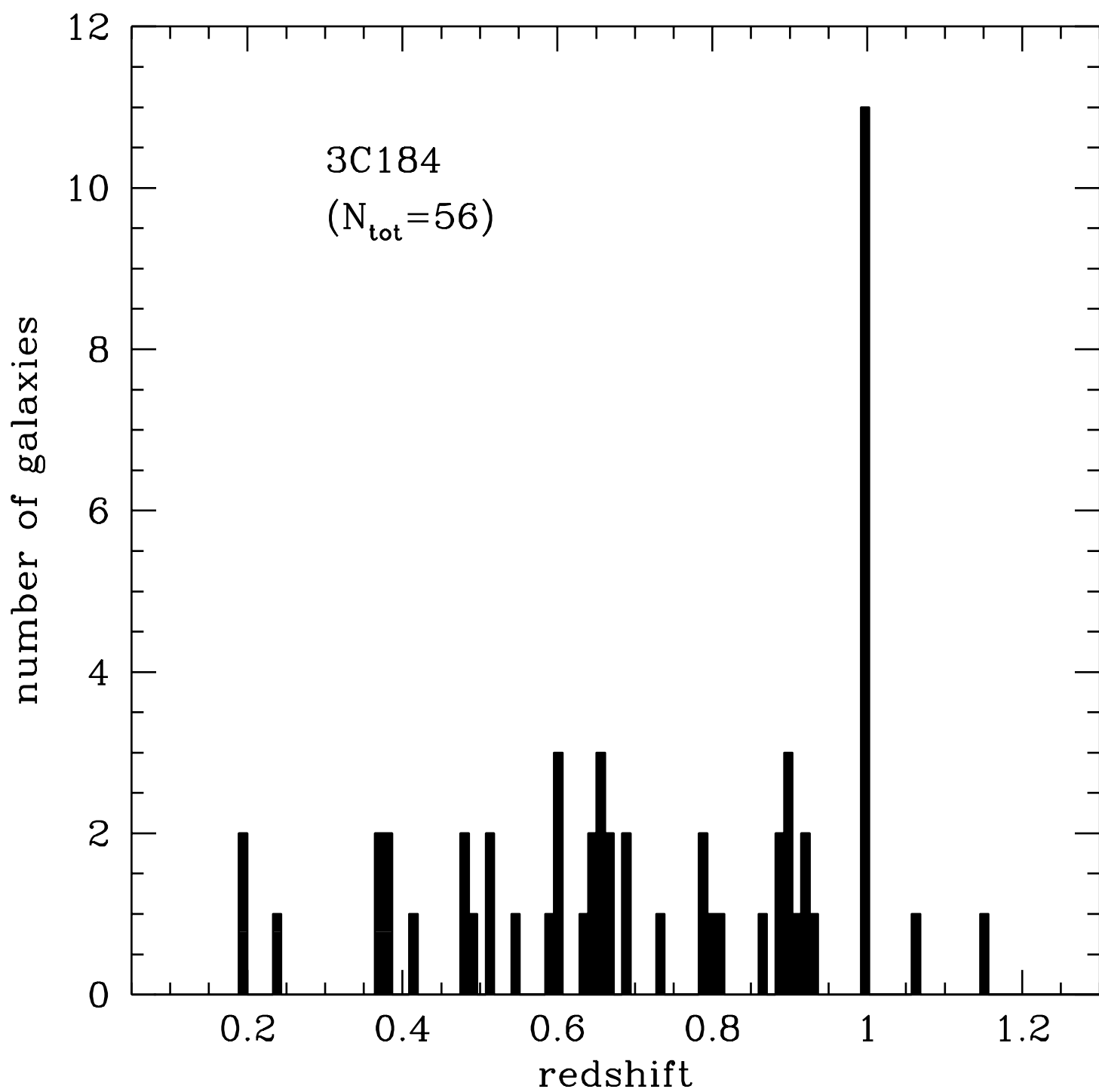


Table 1. Properties of the cluster galaxies

| Object<br>(catalogue number) | $\alpha_{1950}$                                    | $\delta_{1950}$ | I<br>(mag) | redshift | velocity from<br>3CR184 (km s <sup>-1</sup> ) | C <sup>a</sup> | identified features                     |
|------------------------------|----------------------------------------------------|-----------------|------------|----------|-----------------------------------------------|----------------|-----------------------------------------|
| 413                          | 07 <sup>h</sup> 33 <sup>m</sup> 34.38 <sup>s</sup> | 70° 31' 06''8   | 22.1       | 0.9951   | -90                                           | 3              | 3933 3969 4000 4101 4340                |
| 478 <sup>b</sup>             | 07 <sup>h</sup> 33 <sup>m</sup> 52.52 <sup>s</sup> | 70° 29' 51''4   | 21.7       | 0.9919   | -570                                          | 9              | 3727                                    |
| 490 <sup>b</sup>             | 07 <sup>h</sup> 34 <sup>m</sup> 02.06 <sup>s</sup> | 70° 29' 58''3   | 21.4       | 0.9952   | -75.1                                         | 3              | 3727 4861 4959 5007                     |
| 493                          | 07 <sup>h</sup> 33 <sup>m</sup> 41.54 <sup>s</sup> | 70° 29' 59''2   | 22.1       | 1.0021   | 960                                           | 9              | 3727                                    |
| 495(3CR184) <sup>b</sup>     | 07 <sup>h</sup> 33 <sup>m</sup> 59.10 <sup>s</sup> | 70° 30' 01''1   | 19.6       | 0.9957   | 0                                             | 4              | 2799 3346 3727 3868 4340 4861 4959 5007 |
| 555                          | 07 <sup>h</sup> 34 <sup>m</sup> 05.41 <sup>s</sup> | 70° 30' 40''5   | 21.9       | 0.9936   | -315                                          | 3              | 3727 3969                               |
| 602                          | 07 <sup>h</sup> 34 <sup>m</sup> 22.38 <sup>s</sup> | 70° 31' 06''5   | 20.5       | 0.9920   | -556                                          | 3              | 3933 4101 4340 4861                     |
| 697                          | 07 <sup>h</sup> 33 <sup>m</sup> 47.70 <sup>s</sup> | 70° 31' 30''4   | 21.5       | 1.0037   | 1198                                          | 9              | 3727                                    |
| 1131                         | 07 <sup>h</sup> 34 <sup>m</sup> 16.58 <sup>s</sup> | 70° 29' 44''8   | 22.0       | 0.9906   | -750                                          | 3              | 3727 5007                               |
| 1165                         | 07 <sup>h</sup> 33 <sup>m</sup> 43.82 <sup>s</sup> | 70° 29' 34''4   | 22.2       | 0.9941   | -240                                          | 3              | 3727 3969 5007                          |
| 1168                         | 07 <sup>h</sup> 33 <sup>m</sup> 39.28 <sup>s</sup> | 70° 30' 25''3   | 20.4       | 0.9928   | -436                                          | 3              | 3727 3933 5007                          |

<sup>a</sup>Confidence class of spectroscopic identification, as in Le Fèvre et al. 1995

<sup>b</sup>object within HST field